Workshop on Virtual Reality Interaction and Physical Simulation VRIPHYS (2014)
J. Bender, C. Duriez, F. Jaillet, and G. Zachmann (Editors)

Coupling Hair with Smoothed Particle Hydrodynamics Fluids

Wei-Chin Lin

TWR Entertainment, Inc.

Abstract

We present a two-way coupling technique for simulating the complex interaction between hair and fluids. In our approach, the motion of hair and fluids is simulated by evaluating the hydrodynamic forces among them based on boundary handling techniques used in SPH (Smoothed Particle Hydrodynamics) fluids. When hair makes contact with fluids, water absorption inside the hair volume can be simulated with a diffusion process by treating the hair volume as porous media with anisotropic permeability. The saturation of each hair strand is then used to derive the adhesive force between wet hair strands. This enables us to simulate the formation of hair clumps dynamically without the need to employ post clumping processes. The proposed method can be easily applied to any SPH fluid solvers as well as various hair models.

Categories and Subject Descriptors (according to ACM CCS): I.3.5 [Computer Graphics]: Computational Geometry and Object Modeling—Physically Based Modeling

1. Introduction

While hair-fluid interaction has become more and more common in the movie industry, those results are usually created using several iterations of a two-pass methodology: first the fluids are simulated in a fluid solver then the results are used as obstacles for the simulation of the motion of hair (and vice versa). However, some important details, including the modification of hair properties from dry to wet, underwater hair dragging and dynamic hair clump formation, are missing. To simulate these complex interactions between fluids and deformable solids, a two-way hair-fluid coupling technique with proper hydrodynamic force models is required. Moreover, a self-adhesion model for wet hair strands is necessary for dynamic hair clump formation if no fluid particles are in the vicinity of these wet hair strands.

In recent years, two-way coupling techniques have been developed for simulating the interaction between lagrangian fluids and deformable solids. These techniques successfully capture the small scale phenomena between fluids and solids. For instance, Akinci et al. [AIA*12] sampled rigid or deformable solids [ACAT13] with boundary particles, then computed the representative volume of boundary particles for fluid density correction and pressure computation. This results in some impressive interactions between rigid bodies, cloth and fluids.

Although these techniques seem to be applied to hair-fluid coupling directly, once some fluid particles are trapped between the volume of hair, large fluid pressure forces will be evaluated, resulting in unstable simulation. To address the stability issue, we propose to manipulate the hydrodynamic forces between hair and fluids using the wetness of hair strands which is calculated by considering the fluid flow inside hair volume.

Rungjiratananon et al. [RKN12] introduced a Cartesian grid to represent the dynamic capillary system for water absorption inside hair volume. However, the force transfer between fluids and hair strands is not clearly described in their work. Moreover, their method seems to be limited to some specific hairstyles only. Lenaerts et al. [LAD08] exploited porous particles and model the evolution of absorbed fluid mass using SPH to simulate porous flow at a macroscopic scale. Our fluid absorption method is similar to the one described in [LAD08]. Instead of using an isotropic permeability in the fluid absorption process, an anisotropic one is used to better approximate the structure of the void space inside hair volume.

In this paper we propose a method to manipulate the forces between fluids and hair. Our method extends the boundary handling technique that previously was used for solid-fluid coupling [AIA*12] by incorporating a diffusion process before fluid force computation. The wetness of hair strands is used to attenuate fluid pressure force, resulting in a

© The Eurographics Association 2014.

DOI: 10.2312/vriphys.20141229

delivered by EUROGRAPHICS DIGITAL LIBRARY www.eg.org diglib.eg.org

stable hair-fluid interaction. For dynamic hair clump formation, the proposed hair self-adhesive force allows us to simulate the sticking effects for various hairstyles. Moreover, our self-adhesive force can be added to existing post clumping procedure to enhance the realism. Combining these, we are able to simulate a variety of challenging scenarios such as the transition from dry to wet hair, gradual hair submerging and clump formation when hair is leaving water surface (Figure 6). Furthermore, our method is generic and therefore can be easily added to existing fluid and hair solvers.

The rest of the paper is composed as follows: Section 2 briefly discusses other works related to hair-fluid coupling. Section 3 explains how the hydrodynamic forces are exchanged between hair and fluids by considering water absorption inside hair volume. Section 4 introduces the dynamic hair clumping process. Section 5 shows some experimental results of the proposed hair-fluid coupling technique. Section 6 discusses the limitations of our method before the conclusion in Section 7.

2. Related Work

In this section, we briefly discuss some of the many techniques that have been proposed for the interaction between deformable solids and lagragian fluids. Please note that in the following context, we call a sampled particle used for hair-fluid coupling on each hair segment *hair boundary particle*, as illustrated in Figure 1(c).

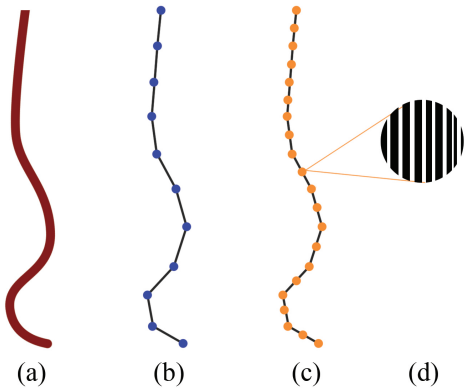

Figure 1: *The discretization (b) of a hair strand (a) and the sampled hair boundary particles (c) used in fluid force evaluation and fluid absorption. Each hair boundary particle is also treated as porous particle for the fluid absorption process (d).*

2.1. Two-Way Rigid-Fluid Coupling in SPH Fluids

Boundary handling is a crucial step for a two-way solid-fluid coupling technique. A commonly used technique is the distance-based penalty method [MST*04, Mon05, HKK07, MK09]. However, these approaches suffer from sticking artifacts. Although Harada et al. [HKK07] proposed a wall weight function to alleviate the sticking artifacts in these approaches, a small time step is required to achieve stable simulation because large penalty force is used. The sticking particle issues can be alleviated either by frozen and ghost particles as proposed by [Lib91, HA06, DK01, IAGT10]. In their approaches, the relevant field variables are well approximated by sampling the boundary with fluid particles, resulting in continuous pressure gradients that prevents fluid particles from sticking to the boundaries. However, for fluid interacting with thin-shells or rods, fluid particles on both sides of the boundary affect each other in their approaches.

Akinci et al. [AIA*12] proposed a boundary handling method that successfully alleviates particle sticking artifacts by including boundary particles in fluid density estimation. In their approach, however, the diameter of rods as well as the thickness of shells cannot be smaller than the diameter of a fluid particle. In our approach, the fluid pressure force on each colliding hair boundary particle is attenuated by its wetness. As a result, two neighboring hair strands can move as closely as possible if a fluid particle is sandwiched between them. In other words, fluid particles are allowed to move through the volume of hair.

For the two-way rigid-fluid coupling, Clavet et al. [CBP05] considered the fluid particles as rigid spheres that exchange impulses with surrounding rigid bodies. In [KAD*06, ODAF06], the pressure at the boundary is taken into account for two-way coupled fluid-rigid interaction. In those models, however, viscosity is neglected. Oh et al. [OKR09] proposed an impulse-based approach to solve rigid body interaction in SPH. However, this approach relies on normal information of rigid bodies and does not guarantee non-penetration for thin boundaries.

Hadap et al. [HMT01] proposed to treat hair as fluids (*hair fluid*) and used SPH to simulate hair dynamics. In their work, the air drag is simulated using two fluids, air and hair, and controlled by the drag coefficient. However, no actual fluid particles exist to exert hydrodynamic forces to neighboring hair strands.

In [AAT13], a surface tension model and a fluid-solid adhesion model are proposed to improve the treatment of fluid-air and fluid-solid interfaces. Their approach can handle large surface tensions by minimizing surface area in all scales while conserving momentum. In this paper, we adopt the adhesion model used in [AAT13] for handling the fluid-hair interfaces. In addition, we apply similar cohesion forces to wet hair boundary particles to model self-adhesive force between neighboring hair strands to simulate dynamic hair clump formation.

© The Eurographics Association 2014.

2.2. Porous Flow in SPH Fluids

Researchers outside the field of computer graphics have studied fluid flow through porous media. Sawley [SCH99] presented an SPH framework in which porous media are modeled by fixed particles in the fluid domain. [MFZ97, ZFM99] extend SPH to allow incompressible porous flow. Although these methods produce accurate results, modeling porous flow at a pore scale using SPH is too expensive for hair-fluid coupling. Lenaerts et al. [LAD08] treated the pores at a macroscopic scale and reused the particle representation of the deformable objects to model the diffusion process within porous materials. Similar to [LAD08], we sample several hair boundary particles on each rod segment for the boundary handling and the diffusion process. Moreover, we extend their work by adopting anisotropic permeability in our diffusion process to model the directional fluid flow along void spaces in hair volume.

2.3. Wetting Effects in Hair Simulation

Since one of the most obvious visual appearances of wet hair is the sticking effect of neighboring hair strands, there were methods proposed to simulate wet hair motion and the formation of hair clumps. In [RKN12], an Eulerian approach is used for capturing the microscopic porosity of hair to simulate water absorption and diffusion, cohesion of wet hair strands, water flow within the hair volume and water dripping from the wet hair strands. However, they did not address the force transfer between hair and fluid. Therefore, the dynamics of fluid and hair do not match properly. In [WL04], hair clumping is created by decreasing the radii of hair segments on their dual-skeleton model. Although a dynamic bonding mechanism between skeletons is included, the clumping effect of wet hair only exists in a single global skeleton. Bruderlin et al. [Bru99] proposed a map-based method to generate wet and broken-up animal fur. Although this technique has successfully been used in some feature films, it is suitable for short fur only.

We simulate the wetting effects by decreasing the elastic moduli of the rods using the saturation of each hair boundary particle. Furthermore, we propose to model the adhesive forces between neighboring strands using SPH to achieve dynamic hair clump formation.

3. Hair-Fluid Interaction

This section elaborates the key steps of our hair-fluid coupling method. Section 3.1 describes how we simulate the fluid flow inside hair volume. Section 3.2 introduces the transfer of the hydrodynamic forces between hair and fluid, including pressure, viscous and adhesive forces.

3.1. Porous Flow in Hair Volume

Similar to [LAD08], the fluid flow inside hair volume is simulated at a macroscopic scale in this paper. Several porous particles are sampled on each segment of the discretized hair strands (Figure 1(b)). Each porous particle p_i contains mass m_i, volume V_i, porosity ϕ_i and permeability $\mathbf{K}_i$. ϕ_i represents the volume fraction of the void space for the hair segment to absorb fluid, therefore, $\phi_i V_i$ represents the volume of the void space. Due to the thin structure of each hair fiber, the hair volume should be treated as an anisotropic permeable medium. Therefore, a second-order symmetric tensor is used to represent the permeability $\mathbf{K}_i$ of each porous particle. In this paper, a small value (0.02) is used for the off-diagonal elements in $\mathbf{K}_i$. Figure 2 illustrates the water absorption effect of using an anisotropic permeability comparing with that of using an isotropic permeability.

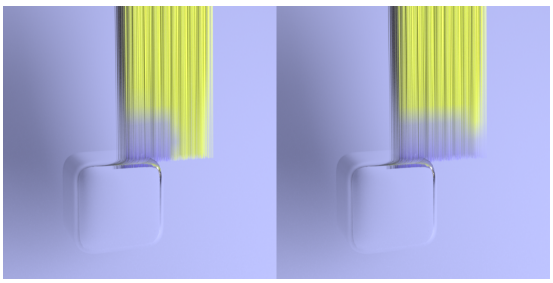

Figure 2: *The comparison between the results using anisotropic (left) and isotropic (right) permeability. Fluid dynamics and fluid-hair interactions are turned off in this example to amplify the diffusion effect.*

In [LAD08], they applied Darcy law [Dar56] derived from the general Navier-Stokes equations, relating the pressure gradient ∇P, the viscosity μ on a fluid and the permeability $\mathbf{K}$ to a volumetric flux density. This Darcy flux is then related to the pore velocity $\mathbf{v}_p$ by dividing by the porosity ϕ:

$$\mathbf{v}_{pi} = -\frac{\mathbf{K}_i}{\phi_i \mu}(-\nabla P_i^c - \rho_i g), \tag{1}$$

where ρ_i is the density of each porous particle, g is the gravitational acceleration and ∇P_i^c is the gradient of the capillary potential computed using SPH:

$$\nabla P_i^c = -\sum_j V_{diffuse\_b_j} P_j^c \nabla W(\mathbf{x}_j - \mathbf{x}_i, h_j), \tag{2}$$

where $P_j^c = k^c(1\text{-}S_j)^\alpha$ is the capillary potential defined by the saturation of the porous particle S_j and controlled by a constant k^c and α. For all examples in this paper, α is set to 0.5. Notice that we do not include the pore pressure P^p as described in [LAD08] because the hair boundary particles on a strand do not compress (due to the inextensibility of the hair) and we are using an anisotropic permeability with small off-diagonal elements such that the pore pressure caused by the compression of neighboring hair strands

© The Eurographics Association 2014.

is negligible. $V_{diffuse\_b_j}$ (defined in Section 3.2) is the representative hair boundary volume for the diffusion process and only hair boundary particles are included to compute $V_{diffuse\_b_j}$. The saturation of a porous particle is

$$S_i = \frac{m_i}{\rho_0 \phi_i V_{diffuse\_b_i}} \tag{3}$$

where ρ_0 is the fluid rest density which is typically 1000 kg/m^3.

The pore velocity field in Equation (1) controls the anisotropic diffusion inside the hair volume. The evolution of the absorbed fluid mass is computed in an Eulerian way by using the SPH approximation to the diffusion equation as described in [MSKG05]:

$$\frac{\partial m_i}{\partial t} = \sum_j d_{ij} V_{diffuse\_b_j} m_j \nabla^2 W(\mathbf{x}_j - \mathbf{x}_i, h_j), \tag{4}$$

where d_{ij} is the diffusion coefficient [LAD08] between two particles. It is proportional to the direction and length of the pore velocity.

$$d_{ij} = \mathbf{v}_{pj} \frac{\mathbf{x}_j - \mathbf{x}_i}{|\mathbf{x}_j - \mathbf{x}_i|} S_j^{\gamma} \tag{5}$$

where γ is a constant that controls this flow. γ is set to 7.0 for all examples in this paper.

The fluid mass is then integrated in time using an explicit Euler integration step:

$$m_i = m_i + \Delta t \frac{\partial m_i}{\partial t} \tag{6}$$

In our implementation, the fluid particles that are in the neighborhood of hair strands are also treated as porous particles. These fluid particles are included for the computation in the diffusion process (Equations 1-6). They are gradually shrinking and are deleted until they reach the minimum size (10% of the original size in all our examples). We use [DC99] to apply symmetric pressure forces to variable sized fluid particles. Unlike [LAD08], we do not emit fluid particles because the hair volume is drastically changing and there are no real inside/outside regions of the volume to be determined for fluid emission. Nevertheless, the fluid emission is one of our future work.

3.2. Fluid-Hair Force Transfer

For the force transfer between hair and fluid, we reuse the porous particles that we generated previously and treat them as boundary particles for boundary handling. Similar to [AIA*12], the representative volume of each boundary particle $V_{b_i}=\frac{1}{\sum_k W_{ik}}$ is used to correct the density of each fluid particle and compute the fluid-solid forces, where k denotes the boundary particle neighbors and $W_{ik} = W(\mathbf{x}_i\text{-}\mathbf{x}_k, h)$ denotes the Gaussian-like kernel function with supporting radius h.

The pressure force exerted from a boundary particle b_k to a fluid particle f_i is

$$\mathbf{F}^p_{f_i \leftarrow b_k} = -m_{f_i} a_{b_k} \Psi_{b_k}(\rho_0) \left(\frac{p_{f_i}}{\rho^2_{f_i}} \right) \nabla W_{ik}, \tag{7}$$

where m_{f_i} is the mass of fluid particle f_i and $a_{b_k}=(1\text{-}S_k)$ is the attenuation factor controlled by the saturation S_k of hair boundary particle b_k. $\Psi_{b_k}(\rho_0)=\rho_0 V_{b_k}$ is used to replace the mass of a boundary particle. The viscous force is

$$\mathbf{F}^v_{f_i \leftarrow b_k} = -m_{f_i} \Psi_{b_k}(\rho_0) \Pi_{ik} \nabla W_{ik}, \tag{8}$$

where Π_{ik} is the laminar artificial viscosity model used in [Mon05, BTT09]. The adhesive force between fluid particles and boundary particles is

$$\mathbf{F}^{adhesion}_{f_i \leftarrow b_k} = -\beta m_{f_i} \Psi_{b_k}(\rho_0) A(|\mathbf{x}_i - \mathbf{x}_k|) \frac{\mathbf{x}_i - \mathbf{x}_k}{|\mathbf{x}_i - \mathbf{x}_k|} \tag{9}$$

where A is a spline function created in [AAT13]:

$$A(r) = \frac{0.007}{h^{3.25}} \begin{cases} \sqrt[4]{-\frac{4r^2}{h} + 6r - 2h} & 2r > h \wedge r \le h \\ 0 & \text{otherwise.} \end{cases} \tag{10}$$

In this formulation, fluid particles are allowed to penetrate through the volume of a set of wet hair strands (Equation (7)). The motion of completely wet hair strands is therefore driven by viscous and adhesive forces only.

Finally, the forces from fluid particles to hair boundary particles are symmetric: $\mathbf{F}^p_{b_k \leftarrow f_i} = \text{-}\mathbf{F}^p_{f_i \leftarrow b_k}$, $\mathbf{F}^v_{b_k \leftarrow f_i} = \text{-}\mathbf{F}^v_{f_i \leftarrow b_k}$, $\mathbf{F}^{adhesion}_{b_k \leftarrow f_i} = \text{-}\mathbf{F}^{adhesion}_{f_i \leftarrow b_k}$. These forces are then applied to the endpoints of each hair segment, weighted by the barycentric coordinates of the hair boundary particles on the segment as described in [BFA02].

4. Clumping Effect in Wet Hair

Although the fluid-hair adhesive force described in Section 3 may make nearby hair boundary particles stick together, in practice, this adhesive force is not suitable for thin hair strands because the radius of each hair is usually much smaller than that of a fluid particle. Moreover, when hair strands are leaving the fluid surface, there will be no fluid particles in their vicinity to make nearby hair stick together.

© The Eurographics Association 2014.

Therefore, the adhesive force between hair boundary particles needs to be modeled separately.

4.1. Hair Self-Adhesion

Due to the inter-molecular forces of the fluid, wet hair strands stick with each other and form clumps. In this paper, the hair self-adhesive force is modeled by applying a cohesion force similar to the one described in [AAT13]:

$$\mathbf{F}^{clumping}_{b_i \leftarrow b_j} = -\delta \bar{S} U^{atten} \Psi_{b_i} \Psi_{b_j} C(|\mathbf{x}_i - \mathbf{x}_j|) \frac{\mathbf{x}_i - \mathbf{x}_j}{|\mathbf{x}_i - \mathbf{x}_j|}, \quad (11)$$

where δ is the self-adhesion coefficient, $\bar{S}$ is the average saturation of hair boundary particles b_i and b_j, U^{atten} is the attenuation factor for hair strands that are underwater as described in Section 4.2. C is a spline function

$$C(r) = \frac{32}{h^9} \begin{cases} (h-q)^3 q^3 & r > R \wedge r \leq h \\ 0 & \text{otherwise.} \end{cases} \quad (12)$$

The adhesive force should only attract particles between the spacing of two colliding cylinders $R = r_a + r_b$ and the supporting radius h because each segment of the rods are approximated using a cylinder (typically with a small radius for plausible results) for collision detection and contact resolution. Note that q is a function of r and is used to modify the range of the spline function C.

$$q(r) = (r + \frac{h}{2} - R)\frac{R}{h} \quad (13)$$

4.2. Underwater Effect

The adhesive force described above makes nearby hair strands stick together after absorbing water. However, in the real world this is not the case when hair is underwater. Therefore, whether a hair strand is submerged in water or not has to be determined. In the first attempt to resolve this problem, a height field was used to check if a hair boundary particle is below fluid surface. However, this method only works for fluids with relatively flat surface and is not sufficient in the case of fluids that are moving freely. Instead, for each hair boundary particle, the surrounding fluid particles are used to evaluate the fluid density ρ_u using SPH. The ratio between ρ_u and rest fluid density is then used to attenuate the self-adhesive force in Equation (11).

$$U^{atten} = (1 - min(\frac{\rho_u}{\rho_0}, 1)) \quad (14)$$

In practice, this simple method successfully resolves the underwater issue and gives us plausible results as can be seen in the accompanying video. Figure 3 shows the effect of the self-adhesion on curly hair strands.

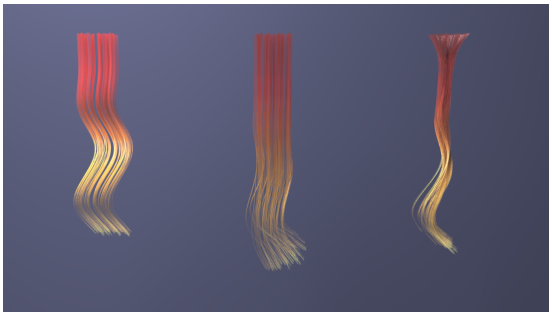

Figure 3: *The comparison of the effects on curly hair strands, (left) without diffusion and self-adhesion, (middle) with diffusion only and (right) with diffusion and self-adhesion.*

5. Implementation

Algorithm 1 presents the pseudo code that summarizes the crucial steps of the proposed hair-fluid coupling method. The techniques described in Section 3 and Section 4 can be added to various SPH fluid solvers easily by following the steps described in Algorithm 1.

Algorithm 1 Hair-Fluid Simulation Step

```
for all fluid particles do
    find fluid and (hair/solid) boundary neighbors
end for
for all (hair/solid) boundary particles do
    find fluid and (hair/solid) boundary neighbors
end for
compute diffusion (§3.1)
for all (hair/solid) boundary particles do
    compute representative volume
end for
for all fluid particles do
    compute density ρ_i
    compute pressure p_i
end for
for all fluid particles do
    compute fluid forces F^{p,v,adhesion} (§3.2)
end for
for all fluid particles do
    update position and velocity
end for
for all hair boundary particles do
    compute self-adhesive force F^{clumping} (§4.1)
end for
transfer hair boundary particle forces to hair vertices
update hair (discrete elastic rods)
```

In this paper, we have implemented the implicit integration of discrete elastic rods [BWR*08, BAV*10] for the simulation of hair dynamics. We use fast projection

© The Eurographics Association 2014.

method [GHF*07] to enforce inextensibility of hair strands, achieving stable hair simulation. Since the fluid forces are treated as external forces on hair strands, our method could also be applied to other hair models, such as [BAC*06, ST07, CJY02, RKN10]. For the collision detection between hair strands and solids, we use spatial hashing method in [THM*03]. For contact resolution between hair strands and solids, we have implemented impulse-based method presented in [BFA02] with slight modifications specifically for one dimensional rods.

We choose the cubic spline kernel function [Mon05] for our SPH simulations. For computing SPH pressures, PCISPH [SP09] is used and the pressure forces that arise from negative pressures are ignored. We use [DC99] to obtain symmetric forces between particles with various smoothing lengths. For adaptive time stepping, we use [IAGT10] and the velocities of boundary particles are also considered to determine the time step. For fluid surface reconstruction, we adopt the method presented in [AIAT12] to obtain smoothing surfaces. In our current implementation, a basic uniform grid is used for neighborhood queries. We plan to utilize parallelism to speedup neighborhood queries by implementing methods such as [IABT11] in the future. Finally, we found sampling each hair segment with 2 hair boundary particles is sufficient to obtain plausible results.

For hair rendering, we employ the multi-lobe hair shading model [SPJT10]. A common approach for the rendering of wet hair is used: the intensity of secondary highlight of a hair strand (that carries the hair color) is attenuated by its wetness to mimic the darkening effects of wet hair. The primary highlight is raised to represent the thin fluid interface on hair fibers.

6. Results

For all of the experiments in this paper, the permeability on main diagonal is $1e^{-11}m^2$. The fluid adhesive coefficient β is 4.0, fluid surface tension is 1.0. The self-adhesive coefficient δ is 0.08 to obtain adequate clumping effects. Thanks to the adaptive time-stepping, the time step for fluid and hair simulation is in a reasonable range. For instance, the time step for the simulation of the sequence in Figure 6 is between $4.3 \cdot 10^{-4}$ and $2.08 \cdot 10^{-3}$.

We start with a brush consisting of straight hair strands submerging into water. When contacting a water surface, some hair strands stick to each other after absorbing water. For those hair strands with full fluid neighborhood, the self-adhesive force between hair strands is nearly negligible. The brush is then lifted to demonstrate the clump formation, as shown in Figure 4.

The same setting is applied to a brush consisting of curly strands. Figure 5 shows a curly brush falling on a fluid surface. Notice that no clump effects exist when the brush is underwater. When the brush is lifted, hair strands tend to stick to their neighboring strands due to the adhesive force. Moreover, wet hair strands are straightened due to the reduced elastic modulus.

Figure 6 shows a furball consisting of 2636 hair strands interacting with water pouring into a container. As the water level gets higher and higher, the furball is gradually submerged in water. Finally clumps form on wet strands after the furball is lifted from water surface. Thanks to the treatment on the fluid pressure force in Equation (7), the system remains stable even in this challenging scenario.

Finally, Figure 7 shows water pouring on a human character consisting of 779 hair strands. With our manipulation of fluid pressure force exerted on hair strands and robust collision handling for elastic rods, the simulation remains stable during the whole process. Due to the proposed self-adhesive force, hair clumps form plausibly when water is gone, as can be seen in Figure 8.

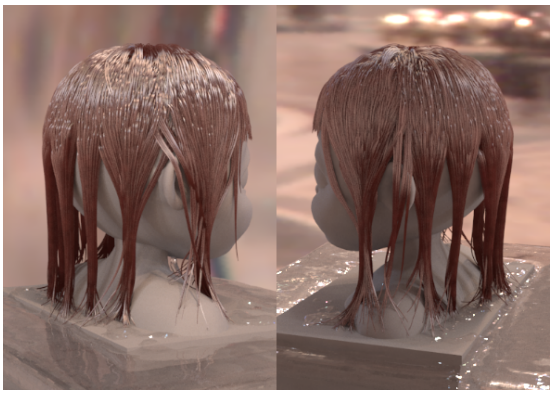

Figure 8: *Hair clumps form dynamically due to the proposed self-adhesive force when water is gone.*

7. Discussion and Future Work

We have integrated our method into both iterative [SP09] and pressure projection fluid solvers [ICS*14]. Despite the stable simulation we have demonstrated in Section 6, we still encounter stability issues on both our fluid and hair solvers. Firstly, if we are simulating highly stiff rods, hair will oscillate violently, which causes large pressure forces on surrounding fluid particles. Therefore, a rather small time step may be required to handle this situation. Secondly, if the permeability of each hair is too low such that hair absorbs fluid slowly, fluid particles may exert extremely large pressure forces on contacting hair strands, resulting in an unstable hair simulation. We plan to address the stability issues between two systems by investigating recent contact handling techniques [DBDB11, KTS*14] and SPH advances [IOS*] in the future.

There are other limitations in our current implementation.

© The Eurographics Association 2014.

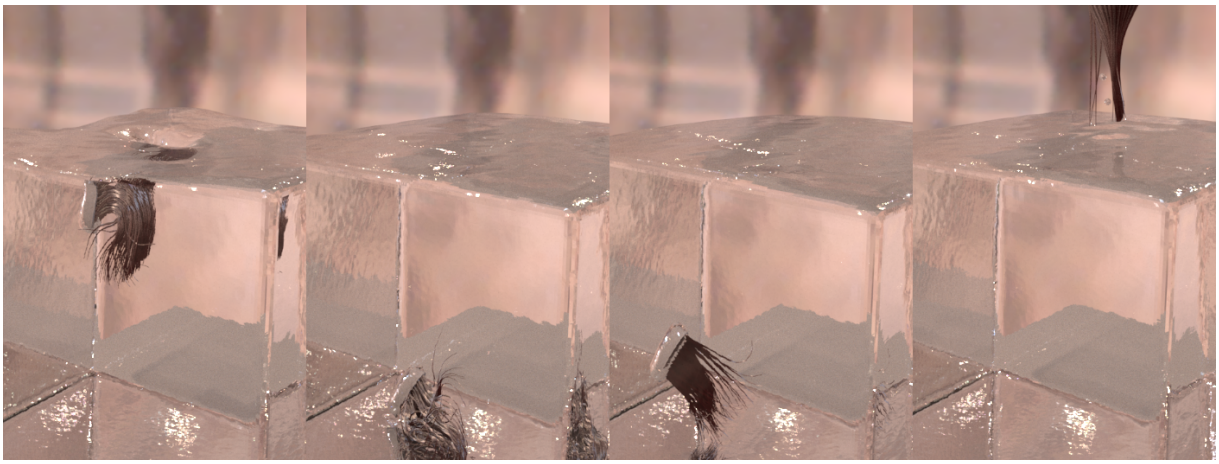

Figure 4: *A brush consisting of 156 straight strands submerged in water.*

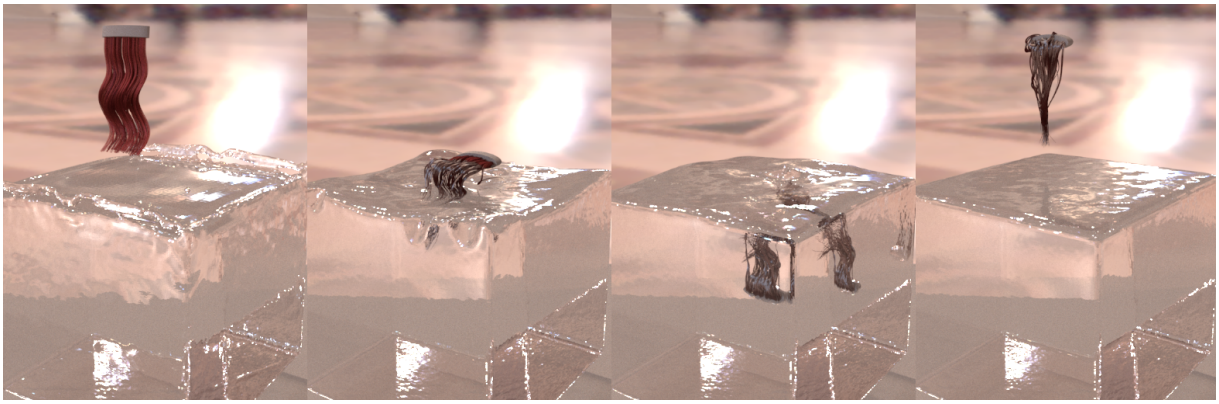

Figure 5: *A brush consisting of 61 curly strands submerged in water.*

First, since the fluid particles are allowed to shrink in the diffusion process, we have to sample solids according to the size of the smallest fluid particle to prevent fluid particles from penetrating through solid boundaries. This results in a large amount of boundary particles in our system and therefore a long simulation time. Second, our self-adhesive force cannot handle hair strands that are thicker than the SPH supporting radius used in fluid dynamics. Fortunately, we didn't encounter this issue since the hair radius is much smaller than the supporting radius in our experiments. However, if this is not the case, we can sample the bounding cylinder of each segment on a hair strand with boundary particles to apply our adhesive force. Third, water dripping can not be simulated since we did not emit fluid particles in the diffusion process. We believe water dripping from hair volume can greatly enhance the visual quality of the simulation. Therefore, it will be one of our future work.

8. Conclusion

We extended boundary handling techniques with porous flow to couple hair with SPH fluids. Our treatment on the hydrodynamic forces using the saturation of hair boundary particles results in physically-plausible simulation. Our hair self-adhesive force makes hair clumps form dynamically and naturally. Therefore, subtle hair-fluid interactions can be realistically reproduced.

References

[AAT13] AKINCI N., AKINCI G., TESCHNER M.: Versatile surface tension and adhesion for sph fluids. *ACM Trans. Graph. 32*, 6 (Nov. 2013), 182:1–182:8. 2, 4, 5

[ACAT13] AKINCI N., CORNELIS J., AKINCI G., TESCHNER M.: Coupling elastic solids with smoothed particle hydrodynamics fluids. *Computer Animation and Virtual Worlds 24*, 3-4 (2013), 195–203. 1

© The Eurographics Association 2014.

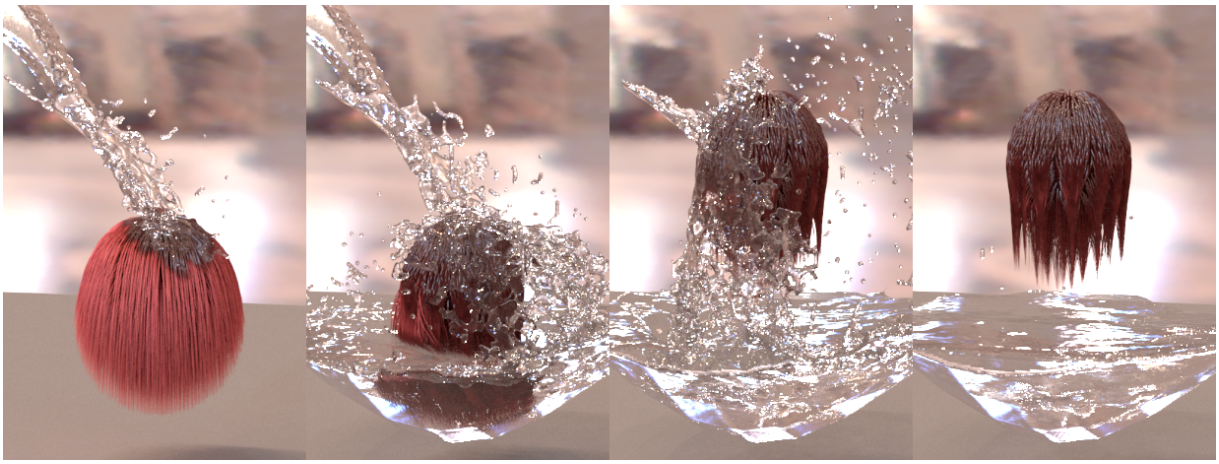

Figure 6: *Water pouring on a furball consisting of 2636 strands. The furball is submerged in water gradually then lifted to demonstrate the formation of hair clumps.*

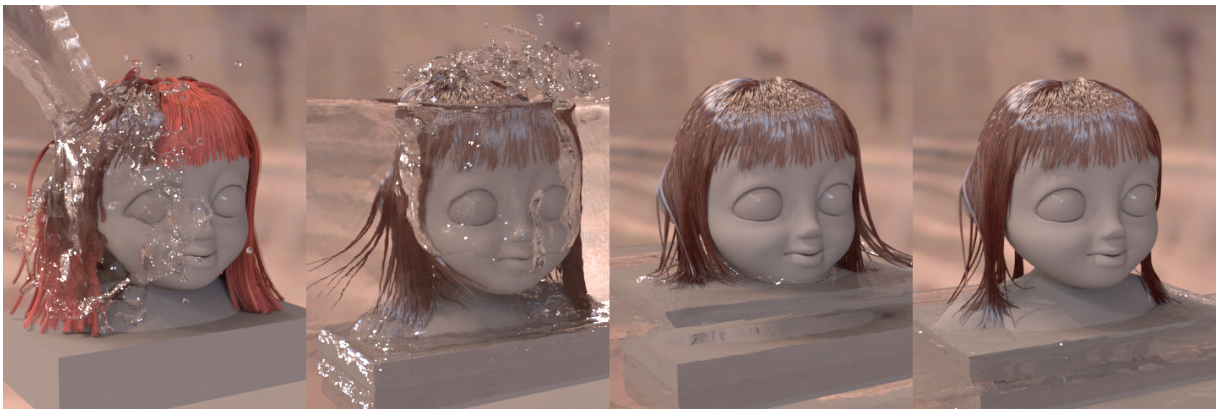

Figure 7: *A character consisting of 779 straight hair strands submerged in water gradually. Clumps form naturally after water is gone.*

[AIA*12] AKINCI N., IHMSEN M., AKINCI G., SOLENTHALER B., TESCHNER M.: Versatile rigid-fluid coupling for incompressible sph. *ACM Trans. Graph. 31*, 4 (July 2012), 62:1–62:8. 1, 2, 4

[AIAT12] AKINCI G., IHMSEN M., AKINCI N., TESCHNER M.: Parallel surface reconstruction for particle-based fluids. *Comput. Graph. Forum 31*, 6 (2012), 1797–1809. 6

[BAC*06] BERTAILS F., AUDOLY B., CANI M.-P., QUERLEUX B., LEROY F., LÉVÊQUE J.-L.: Super-helices for predicting the dynamics of natural hair. *ACM Trans. Graph. 25*, 3 (July 2006), 1180–1187. 6

[BAV*10] BERGOU M., AUDOLY B., VOUGA E., WARDETZKY M., GRINSPUN E.: Discrete viscous threads. In *ACM SIGGRAPH 2010 papers* (New York, NY, USA, 2010), SIGGRAPH '10, ACM, pp. 116:1–116:10. 5

[BFA02] BRIDSON R., FEDKIW R., ANDERSON J.: Robust treatment of collisions, contact and friction for cloth animation. *ACM Trans. Graph. 21*, 3 (July 2002), 594–603. 4, 6

[Bru99] BRUDERLIN A.: A method to generate wet and broken-up animal fur. In *Proceedings of the 7th Pacific Conference on Computer Graphics and Applications* (Washington, DC, USA, 1999), PG '99, IEEE Computer Society, pp. 242–. 3

[BTT09] BECKER M., TESSENDORF H., TESCHNER M.: Direct forcing for lagrangian rigid-fluid coupling. *IEEE Transactions on Visualization and Computer Graphics 15*, 3 (May 2009), 493–503. 4

[BWR*08] BERGOU M., WARDETZKY M., ROBINSON S., AUDOLY B., GRINSPUN E.: Discrete elastic rods. *ACM Trans. Graph. 27*, 3 (Aug. 2008), 63:1–63:12. 5

[CBP05] CLAVET S., BEAUDOIN P., POULIN P.: Particle-based viscoelastic fluid simulation. In *Proceedings of the 2005 ACM*

© The Eurographics Association 2014.

SIGGRAPH/Eurographics Symposium on Computer Animation (New York, NY, USA, 2005), SCA '05, ACM, pp. 219–228. 2

[CJY02] CHANG J. T., JIN J., YU Y.: A practical model for hair mutual interactions. In *Proceedings of the 2002 ACM SIGGRAPH/Eurographics symposium on Computer animation* (New York, NY, USA, 2002), SCA '02, ACM, pp. 73–80. 6

[Dar56] DARCY H.: *Les Fontaines Publiques de la Ville de Dijon, Dalmont, Paris.* 1856. 3

[DBDB11] DAVIET G., BERTAILS-DESCOUBES F., BOISSIEUX L.: A hybrid iterative solver for robustly capturing coulomb friction in hair dynamics. In *Proceedings of the 2011 SIGGRAPH Asia Conference* (New York, NY, USA, 2011), SA '11, ACM, pp. 139:1–139:12. 6

[DC99] DESBRUN M., CANI M.-P.: *Space-Time Adaptive Simulation of Highly Deformable Substances*. Tech. Rep. RR-3829, INRIA, BP 105 - 78153 Le Chesnay Cedex - France, Feb. 1999. 4, 6

[DK01] DALRYMPLE R., KNIO O.: *SPH Modelling of Water Waves*. 2001, ch. 79, pp. 779–787. 2

[GHF*07] GOLDENTHAL R., HARMON D., FATTAL R., BERCOVIER M., GRINSPUN E.: Efficient simulation of inextensible cloth. *ACM Trans. Graph. 26*, 3 (July 2007). 6

[HA06] HU X., ADAMS N.: A multi-phase sph method for macroscopic and mesoscopic flows. *Journal of Computational Physics 213*, 2 (2006), 844 – 861. 2

[HKK07] HARADA T., KOSHIZUKA S., KAWAGUCHI Y.: Smoothed particle hydrodynamics on gpus. pp. 63–70. 2

[HMT01] HADAP S., MAGNENAT-THALMANN N.: Modeling dynamic hair as a continuum. *Comput. Graph. Forum 20*, 3 (2001), 329–338. 2

[IABT11] IHMSEN M., AKINCI N., BECKER M., TESCHNER M.: A parallel sph implementation on multi-core cpus. *Comput. Graph. Forum 30*, 1 (2011), 99–112. 6

[IAGT10] IHMSEN M., AKINCI N., GISSLER M., TESCHNER M.: Boundary handling and adaptive time-stepping for pcisph. In *VRIPHYS* (2010), Erleben K., Bender J., Teschner M., (Eds.), Eurographics Association, pp. 79–88. 2, 6

[ICS*14] IHMSEN M., CORNELIS J., SOLENTHALER B., HORVATH C., TESCHNER M.: Implicit incompressible sph. *IEEE Transactions on Visualization and Computer Graphics 20*, 3 (Mar. 2014), 426–435. 6

[IOS*] IHMSEN M., ORTHMANN J., SOLENTHALER B., KOLB A., TESCHNER M.: SPH Fluids in Computer Graphics. pp. 21–42. 6

[KAD*06] KEISER R., ADAMS B., DUTRÃL' P., GUIBAS L., PAULY M.: *Multiresolution particle-based fluids*. Tech. rep., ETH Zurich, 2006. 2

[KTS*14] KAUFMAN D. M., TAMSTORF R., SMITH B., AUBRY J.-M., GRINSPUN E.: Adaptive nonlinearity for collisions in complex rod assemblies. *ACM Trans. on Graphics (SIGGRAPH 2014)* (2014). 6

[LAD08] LENAERTS T., ADAMS B., DUTRÉ P.: Porous flow in particle-based fluid simulations. *ACM Trans. Graph. 27*, 3 (Aug. 2008), 49:1–49:8. 1, 3, 4

[Lib91] In *Advances in the Free-Lagrange Method Including Contributions on Adaptive Gridding and the Smooth Particle Hydrodynamics Method*, Trease H., Fritts M., Crowley W., (Eds.), vol. 395 of *Lecture Notes in Physics*. 1991. 2

[MFZ97] MORRIS J. P., FOX P. J., ZHU Y.: Modeling low reynolds number incompressible flows using sph. *Journal of Computational Physics 136*, 1 (1997), 214 – 226. 3

[MK09] MONAGHAN J. J., KAJTAR J. B.: Sph particle boundary forces for arbitrary boundaries. *Computer Physics Communications 180*, 10 (2009), 1811–1820. 2

[Mon05] MONAGHAN J.: Smoothed particle hydrodynamics. *Report on Progress in Physics 68*, 8 (2005), 1703–1759. 2, 4, 6

[MSKG05] MÜLLER M., SOLENTHALER B., KEISER R., GROSS M.: Particle-based fluid-fluid interaction. In *Proceedings of the 2005 ACM SIGGRAPH/Eurographics Symposium on Computer Animation* (New York, NY, USA, 2005), SCA '05, ACM, pp. 237–244. 4

[MST*04] MÜLLER M., SCHIRM S., TESCHNER M., HEIDELBERGER B., GROSS M.: Interaction of fluids with deformable solids: Research articles. *Comput. Animat. Virtual Worlds 15*, 3-4 (July 2004), 159–171. 2

[ODAF06] OGER G., DORING M., ALESSANDRINI B., FERRANT P.: Two-dimensional {SPH} simulations of wedge water entries. *Journal of Computational Physics 213*, 2 (2006), 803 – 822. 2

[OKR09] OH S., KIM Y., ROH B.-S.: Impulse-based rigid body interaction in sph. *Computer Animation and Virtual Worlds 20*, 2-3 (2009), 215–224. 2

[RKN10] RUNGJIRATANANON W., KANAMORI Y., NISHITA T.: Chain shape matching for simulating complex hairstyles. *Computer Graphics Forum 29*, 8 (2010), 2438–2446. 6

[RKN12] RUNGJIRATANANON W., KANAMORI Y., NISHITA T.: Wetting effects in hair simulation. *Computer Graphics Forum 31*, 7 (2012), 1993–2002. 1, 3

[SCH99] SAWLEY M., CLEARY P., HA J.: Modelling of flow in porous media and resin transfer moulding using smoothed particle hydrodynamics. In *Second International Conference on CFD in the Minerals and Process Industries* (1999), pp. 473–478. 3

[SP09] SOLENTHALER B., PAJAROLA R.: Predictive-corrective incompressible sph. *ACM Trans. Graph. 28*, 3 (July 2009), 40:1–40:6. 6

[SPJT10] SADEGHI I., PRITCHETT H., JENSEN H. W., TAMSTORF R.: An artist friendly hair shading system. *ACM Trans. Graph. 29*, 4 (July 2010), 56:1–56:10. 6

[ST07] SPILLMANN J., TESCHNER M.: Corde: Cosserat rod elements for the dynamic simulation of one-dimensional elastic objects. In *Proceedings of the 2007 ACM SIGGRAPH/Eurographics symposium on Computer animation* (Aire-la-Ville, Switzerland, Switzerland, 2007), SCA '07, Eurographics Association, pp. 63–72. 6

[THM*03] TESCHNER M., HEIDELBERGER B., MUELLER M., POMERANETS D., GROSS M.: Optimized spatial hashing for collision detection of deformable objects. pp. 47–54. 6

[WL04] WARD K., LIN M. C.: Modeling hair influenced by water and styling products. In *In International Conference on Computer Animation and Social Agents (CASA)* (2004), pp. 207–214. 3

[ZFM99] ZHU Y., FOX P. J., MORRIS J. P.: A pore-scale numerical model for flow through porous media. *International Journal for Numerical and Analytical Methods in Geomechanics 23*, 9 (1999), 881–904. 3

© The Eurographics Association 2014.